Noname manuscript No.
(will be inserted by the editor)

Traffic-aware Stateless Multipath Routing for Fault-Tolerance in IEEE 802.15.4 Wireless Mesh Networks

**Kiwoong Kwon, Seong Hoon Kim,
Minkeun Ha, and Daeyoung Kim**

Received: date / Accepted: date

1 The shortest path toward the root by root oriented directional tree (RODT)

Root Oriented Directional Tree (RODT) has a feature that always ensures the shortest cumulative ETX toward the root. It is proven by the following theorem.

Theorem 1 *In MP2P traffic, the RODT path is always shorter than or equal to other possible paths in terms of cumulative ETX.*

Proof As shown in Fig. 1, all possible paths destined for the root can be divided into the RODT path and other paths. In this figure, r_i is defined as the i_{th} RODT descendant from r_0, where r_0 is the root of RODT, and M_i is defined as a set of neighbors of r_{i-1} excluding r_i. That is, r_i means an intermediate node for the RODT path and $m_i \in M_i$ indicates those for other paths, namely $r_i = r\_par(r_{i+1})$ and $m_i \in N(r_{i-1}) - r_i$, where i is a natural number.

Based on the initial state, $r\_depth(r_0) = 0$, $r\_depth(r_k)$ can be generalized as follows, where k is a natural number:

Kiwoong Kwon and Daeyoung Kim
Department of School of Computing, Korea Advanced Institute of Science and Technology (KAIST), Daejeon 305-701, Rep. of Korea.
E-mail: kiwoong@kaist.ac.kr, kimd@kaist.ac.kr

Seong Hoon Kim
YBrain, Seongnam, 13487, Rep. of Korea.
E-mail: shkim1980@gmail.com

Minkeun Ha
School of Technology and Health, KTH Royal Institute of Technology, Stockholm SE-100 44, Sweden
E-mail: minkeun.ha@sth.kth.se

$$
\begin{aligned}
&r\_depth(r_0) = 0 \\
&r\_depth(r_1) = \underbrace{r\_depth(r_0) + etx(r_1, r_0)}_{by\ Eq.\ 5\ in\ the\ main\ text} \\
&\leq \{m_1 \in M_1 | r\_depth(m_1) = r\_depth(r_0) + etx(m_1, r_0)\} \\
&\quad \cdots \\
&r\_depth(r_k) = r\_depth(r_{k-1}) + etx(r_k, r_{k-1}) \\
&\leq \{m_k \in M_k | r\_depth(m_k) = r\_depth(r_{k-1}) + etx(m_k, r_{k-1})\}
\end{aligned} \tag{1}
$$

In 1_{st} phase on Eq. 1, we can prove $etx(r_1, r_0) \leq etx(m_1, r_0)$ by showing that a counter example is not true. As a counter example, we assume that $etx(r_1, r_0) > etx(m_1, r_0)$. Based on this, m_1 should become r_1 because r_1 must have the shortest etx toward r_0 among $N(r_0)$ according to the features of RODT. However, m_1 was defined as one of $N(r_0)$ excluding r_1, so that $etx(r_1, r_0) > etx(m_1, r_0)$ is not true. Since $r\_depth(r_0)$ is a constant value of 0 and $etx(r_1, r_0) \leq etx(m_1, r_0)$, we can say that $r\_depth(r_1)$ is always shorter than or equal to $r\_depth(m_1)$; that is, r_1 makes the shortest cumulative ETX path toward r_0 among $N(r_0)$. If the remaining phases are sequentially repeated in this way, we can induce $r\_depth(r_k) \leq r\_depth(m_k)$ at the k_{th} phase ($k > 0$). It implies that this is always true for all k. Therefore, theorem 1 is true.

2 Loop avoidance for enhanced shortcut tree routing (ESTR)

Enhanced Shortcut Tree Routing (ESTR) is not a loop-free routing, so that ESTR should protect the intermediate nodes to select the next hop node making the loop. To deal with this, we define which nodes makes the loop and how the loop is avoidable by proving the following theorems. Firstly, we prove that ESTR is not a loop-free routing as follows.

Theorem 2 *ESTR does not provide loop-free routing in the real wireless environment where link failures occur frequently.*

Proof To prove this theorem, we show that ESTR has the probability to reselect one of the previous nodes as the next-hop node. Fig. 2 shows all possible ESTR paths within the next two hops from any intermediate nodes, where e_i is defined as the i_{th} intermediate node by ESTR, and i is a natural number. Assuming that $e_i = x$ and $td(x, d) = k$, e_{i+1} can be classified as three sets; x_g, x_e, and x_l, where x_g, x_e, and x_l satisfy $td(x_g, d) > td(x, d)$, $td(x_e, d) = td(x, d)$, and $td(x_l, d) < td(x, d)$, respectively. Actually, x_g having bigger td than x must not be chosen as the next hop node of x if all links are stably connected, but all links are prone to failure in real wireless environment; thus, x_g also belongs to the candidate set. That is, x_g can be selected as the next-hop node of x when all links connected to x_e and x_l fail. By this classification, nine sets exist at e_{i+2} ($= 3^2$). Among nine sets, x_{gl}, x_{ee}, and x_{lg} include k in their td ranges ($x_{gl} \geq k$, $x_{lg} \leq k$, $x_{ee} = k$). This means that, if those three sets are selected

as the next-hop node of e_{i+1}, $e_i = \{x\}$ can be re-selected at e_{i+2} because $e_i = \{x\}$ is naturally the neighbor of e_{i+1}, and $td(x, d)$ is k. Since there is the probability that $e_i = \{x\}$ is re-selected at e_{i+2}, ESTR is not the loop-free routing.

For ESTR to avoid routing loop, we have not only to select the three sets; x_{gl}, x_{ee}, and x_{ge}, within next two-hop. However, considering further steps over e_{i+2}, some of the following six sets, x_{ge}, x_{gg}, x_{eg}, x_{le}, x_{ll}, and x_{el}, also make a routing loop or infinite routing. Straightforwardly, to avoid routing loops and infinite routing, each node is required to select the next-hop node whose *td* is smaller than that of every previous two-hop node. This is proved as follows.

Theorem 3 *In ESTR, each node in every hop should select the next-hop node whose td is smaller than that of every previous two-hop node to avoid the formation of a routing loop and infinite routing.*

Proof Fig. 3 shows every possible next two-hop node from e_i by ESTR. Assuming that we initially define $e_i = X = \{x\}$ and $td(X, d) = k$, e_{i+2} can be classified as X_g and X_l which satisfy $td(X_g, d) > td(X, d)$ and $td(X_l, d) < td(X, d)$, respectively. Note that we ignore X_e, which satisfies $td(X_e, d) = td(X, d)$, because it is proved that X_e has the probability to make a routing loop in theorem 2. By this classification, four sets, X_{gg}, X_{gl}, X_{lg} and X_{ll}, exist at e_{i+4}. Among them, since X_{gl} and X_{lg} include k in their *td* ranges, they have probability to re-select X at e_{i+4} and make routing loop; thus, only X_{gg} or X_{ll} should be selected. To generalize this by $j > 2$ where j is natural number, at $e_{i+2\cdot j}$, only X_{xgg} or X_{xll} should be consecutively selected to avoid a routing loop because X_{xgl} and X_{xlg} always include k in their *td* ranges. Of X_{xgg} and X_{xll}, if X_{xgg} is consecutively selected in every step, *td* increases only; that is, infinite routing occurs. In opposite case, *td* decreases so that routing can be finished. This means that only if X_{xll} whose *td* is smaller than that of every previous two-hop node, is selected at every hop, ESTR is free of routing loops and infinite routing.

Theorem 3 shows that ESTR is promising only when the nodes whose *td* values are smaller than that of every previous two-hop node are selected at every next two-hop. Since only $X_l = \{x_{el}, x_{le}, x_{ll}\}$ satisfies the promising condition at e_{i+2} in Fig. 3, only the X_l nodes are considered promising nodes, and the others are considered unpromising nodes. When the unpromising nodes are selected as the next-hop node by ESTR, the unpromising condition, which may make routing loop and infinite routing, can be avoidable by alternatively conducting RODTR.

3 Performance evaluations on the number of sessions

To examine the effect of the number of sessions, we increased the number of sessions from 40 to 80 by increments of 10 under the condition of the fixed network density and size. Consequently, we set total number of nodes 100 and the number of neighbors 15 on average.

3.0.1 P2P Traffic

Fig. 4 (a) shows PDR in P2P traffic. TSMR always provides the highest PDR among others, and the performance degradation is relatively small compared to other. This implies that TSMR is less influenced as the number of sessions increases. Its PDR is at least over 10% higher than others at 80 sessions. Fig. 4 (b) shows the E2E delay in P2P traffic. Here, TSMR surpasses ZTR, STR, and RPL, but slightly falls behind AODV. The reason for this is the same as that shown in Fig. 7 (b) of the manuscript. Fig. 4 (c) and (d) show the control and memory consumption in P2P traffic, respectively. Since their graph trends and descriptions are similar to those shown in Fig. 7 (c) and (d) of the manuscript, respectively, the description is skipped here. Please refer to Section 7.2.1 of the manuscript.

3.0.2 MP2P Traffic

Fig. 5 (a) shows PDR for MP2P traffic. Graph trends are nearly similar to those shown in Fig. 8 (a) of the manuscript, but remarkable difference is that the graph of AODV gradually declines. This implies that AODV is badly influenced by increase in the network size rather than the number of sessions. Fig. 5 (b) shows E2E delay for MP2P traffic. Here, E2E delay of TSMR is obviously shorter than that of AODV. In the case of AODV, since the nodes discover the paths only toward the root, the route request (RREQ) messages frequently collide with each other around the root; thus, the detour path is generated around the root. On the other hands, TSMR provides the nearly optimal path in MP2P traffic due to RODT. Since the graph trends of Fig. 5 (c) and (d) are similar to those shown in Fig. 8 (c) and (d) of the manuscript, respectively, the description is skipped here. Please refer to Section 7.2.2 of the manuscript.

3.0.3 P2MP Traffic

Fig. 6 (a) shows PDR for P2MP traffic. Notable change here is that PDR of TSMR is always higher than that of RPL compared to Fig. 9 (a) of the manuscript. This is because the gap between the average sizes of source routing headers of RPL and TSMR in Fig. 7 widens in comparison of Fig. 10 of the manuscript. The more the header size is big, the more the packets are produced by fragmentation; thus, the packet collisions more often arise. Here, since the descriptions about Fig. 6 (b), (c), and (d) are similar to those shown in Fig. 9 (b), (c), and (d) of the manuscript, the description skipped here. Please refer to Section 7.2.3 of the manuscript.

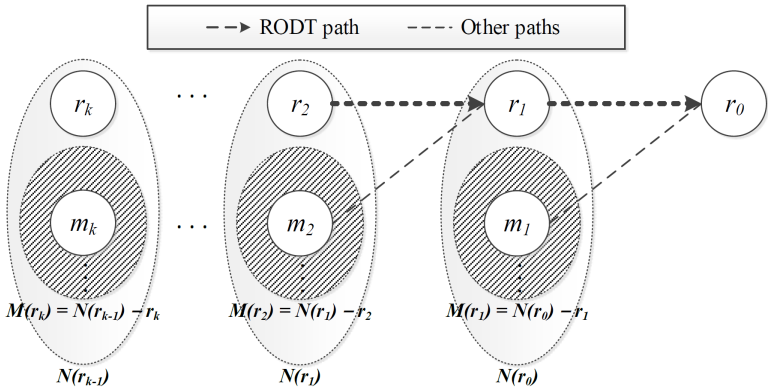

Fig. 1: RODT path and other possible paths toward the root

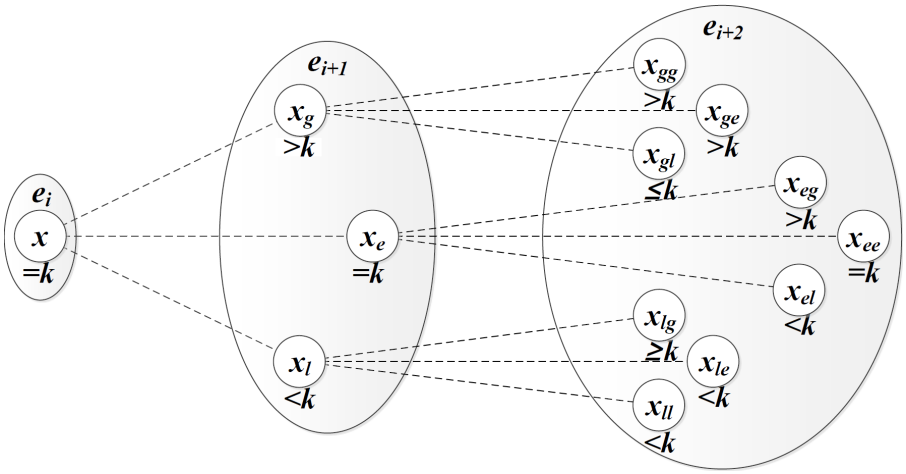

Fig. 2: All possible paths within two hops from e_i by ESTR

Table 1: Notations and their descriptions

Symbol	Description
E	Set of edge
G	Graph
IM	Inconsistency message
M_i	Set of neighbors of r_{i-1} excluding r_i
$N(v)$	Set of neighbors of v
SRP	Source routing path
SRT	Source routing table
V	Set of vertex
$addr(v)$	Address of v
$b\_anc(v)$	BDT ancestor of v
$b\_depth(v)$	BDT depth of v
b_on	BDT orphan node
$b\_par(v)$	BDT parent of v
c	Current intermediate node
d	Destination
$ece(c, n, d)$	Expected cumulative ETX
$etx(v_1, v_2)$	ETX of the edge between v_1 and v_2
e_i	i^{th} intermediate node by ESTR
$lca(v_1, v_2)$	Lowest common ancestor between v_1 and v_2
m	Farthest order of $r\_desc(r\_on)$ from r_on
mc	Maximum number of child degrees
n	One of neighbors
$po(v)$	Position order of v
r_0	Root of RODT
$r\_depth(v)$	RODT depth of v
$r\_desc(v)$	RODT descendant of v
r_i	i^{th} RODT descendant from r_0
r_on	RODT orphan node
$r\_par(v)$	RODT parent of v
$srp(v)$	Source routing path from the root to v
$td(v_1, v_2)$	Tree distance between v_1 and v_2
ve	Virtual ETX of all links excluding neighbors
x_g	Set of neighbors satisfying $td(x_g, d) > td(x, d)$
x_e	Set of neighbors satisfying $td(x_e, d) = td(x, d)$
x_l	Set of neighbors satisfying $td(x_l, d) < td(x, d)$

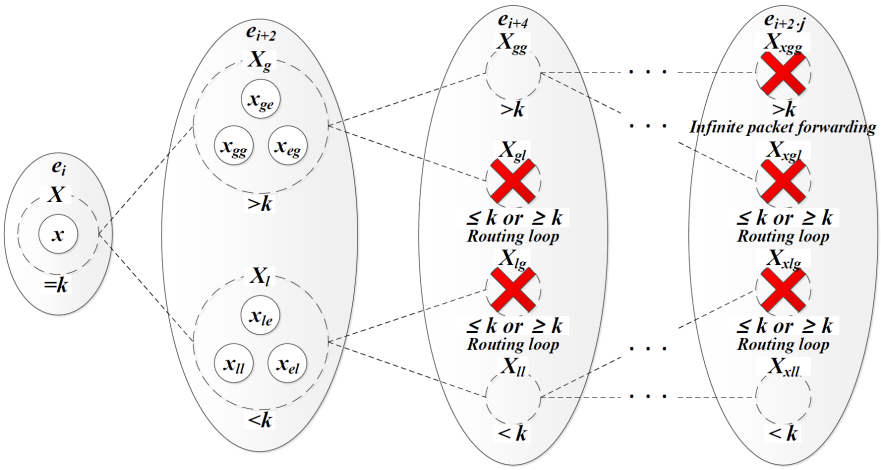

Fig. 3: Every possible next two hop node from e_i by ESTR

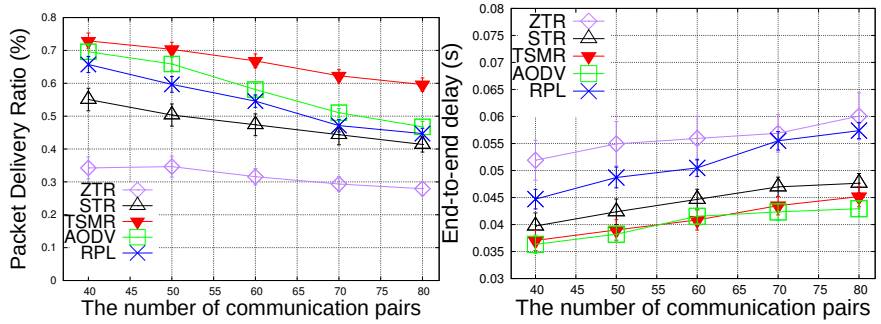

(a) PDR in P2P traffic

(b) E2E in P2P traffic

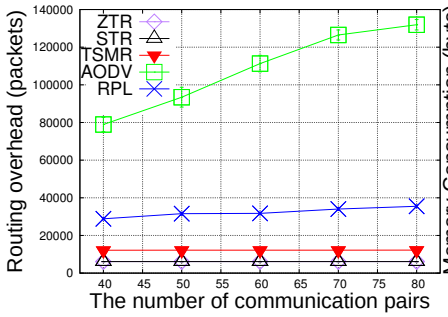

(c) Control Overhead in P2P traffic

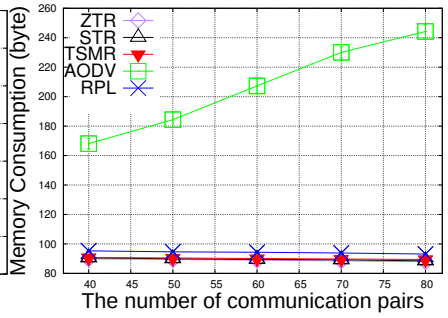

(d) Mem. Consumption in P2P traffic

Fig. 4: Routing performance for packet delivery ratio (a), end-to-end delay (b), control overhead (c), and memory Consumption (d) in P2P traffic as the number of sessions increases

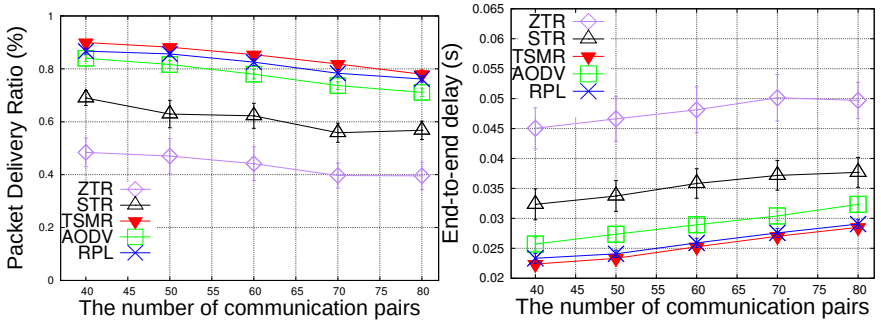

(a) PDRin MP2P traffic

(b) E2E in MP2P traffic

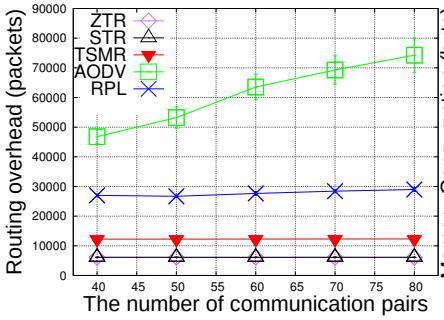

(c) Control Overhead in MP2P traffic

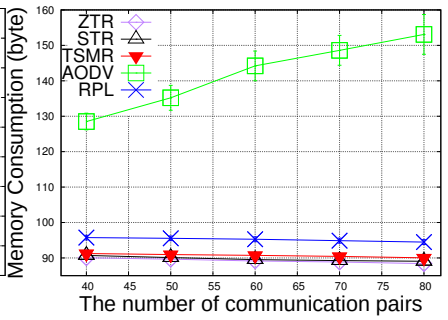

(d) Mem. Consumption in MP2P traffic

Fig. 5: Routing performance for packet delivery ratio (a), end-to-end delay (b), control overhead (c), and memory Consumption (d) in MP2P traffic as the number of sessions increases

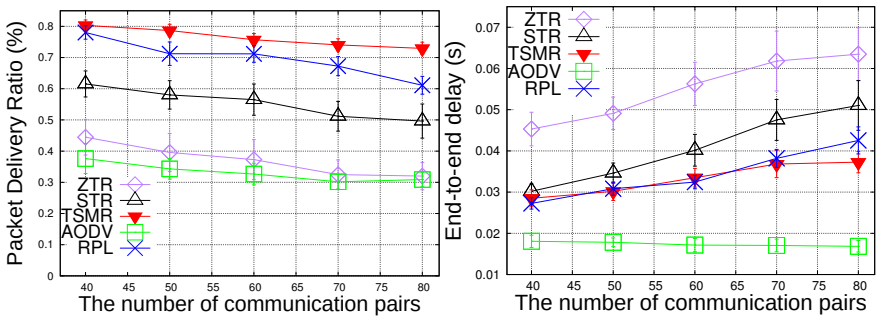

(a) PDR in P2MP traffic

(b) E2E in P2MP traffic

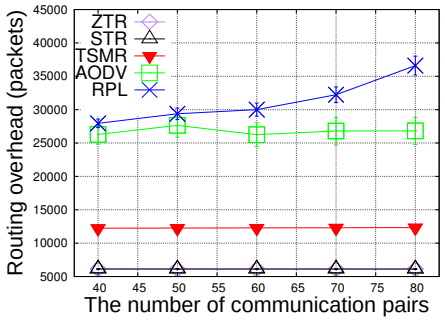

(c) Control Overhead in P2MP traffic

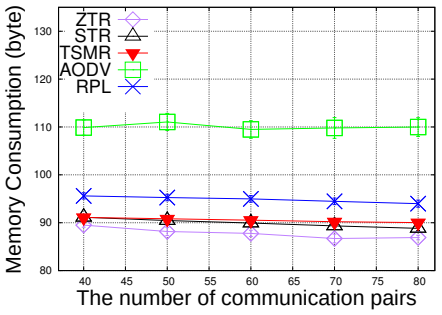

(d) Mem. Consumption in P2MP traffic

Fig. 6: Routing performance for packet delivery ratio (a), end-to-end delay (b), control overhead (c), and memory Consumption (d) in P2MP traffic as the number of sessions increases

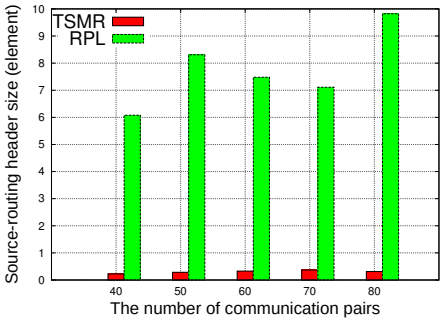

Fig. 7: Comparison of source-routing header sizes of TSMR and RPL as the number of session increases